

EXPERIMENTAL AND NUMERICAL INVESTIGATION OF COMBUSTION BEHAVIOUR IN DIESEL ENGINE FUELLED WITH WASTE POLYETHYLENE OIL

KHATIR NAIMA^{1,2,*}, ABDELKRIM LIAZID^{2,3},
MOHAND TAZEROUD⁴, HAMZA BOUSBA^{2,3}

¹Science Faculty, BP: 66, University Centre of Naama, 45000, Algeria

²LTE Laboratory, BP 1523 El Mnaouer 31000 - Oran, Algeria

³Science Faculty, B.P. 119 - University Abou-Bakr Belkaid, 13000 - Tlemcen, Algeria

⁴IMT-Atlantique Nantes, GEPEA UMR 6144, CNRS, 4 Rue Alfred Kastler,
44307, Nantes, France

*Corresponding Author: n_khatir@hotmail.com

Abstract

The aim of this investigation is to evaluate the usability of waste polyethylene oil as an alternative fuel for diesel engines. The novel fuel is obtained by a pyrolysis process of waste polyethylene at 973 K. The obtained oil is tested in a single cylinder air cooled (TS1) direct injection diesel engine at 1500 rpm. Engine performances and exhaust pollutant emissions from Waste Polyethylene Oil (WPO) were analysed and compared to those obtained from the same engine fuelled with conventional diesel fuel. Results showed that the total fuel consumption of WPO is lower than that of neat diesel fuel due to the higher heating value of WPO. Brake Thermal Efficiency (BTE) is improved for WPO especially at low load. The exhaust gas temperature is lower for WPO than that of diesel at low and full load. CO and UHC are found lower, while NO_x emissions are higher at high loads. Furthermore, the use of numerical investigation permits to optimize the injection parameters, which can help to take advantages of WPO fuel. The simulation results suggest advancing the injection timing.

Keywords: Diesel engine, Emissions, Performances, Polyethylene, Waste.

1. Introduction

Plastics are materials consisting of a standard group of synthetic or natural materials, produced from long molecular chains with carbon as a unique or major element. Plastics are malleable, highly durable, strong, elastic and cheap. This makes plastics a perfect choice for diverse domains as packaging and storage applications [1]. These plastics are widely used in many applications such as fashion, household appliances, automotive products and aerospace [2]. They are still delivering significant societal benefits, including energy and resource savings, the protection and preservation of food and consumer products. They permit innovations that improve healthcare, reduce food spoilage and improve the quality of life [3].

Due to rapid urbanization and economic development, the world's annual production of plastic materials has increased from around 230 million tons in 2005 to nearly 322 million tons in 2015. About 18.5% of global plastic materials were produced in European Union and 27.8% in China [4]. The huge amount of waste plastics results from the demographic and technological growths becomes a serious environmental problem to be thought about [5]. In fact, the major part of post-consumer plastic wastes are currently landfilled or incinerated, this strategy of waste management is not suitable since these wastes are non-biodegradable and the landfill sites are limited [5]. In 2010 about 4.8 to 12.7 million metric tons of waste plastic deposited in the ocean from the coastal countries beaches [6]. The improper disposal of waste plastics has serious consequences on the earth bio-diversity, leading to the death of aquatic animals, widespread of diseases and the affection of soils and their agricultural productivity, which is the beating heart of the national economy of many countries [7].

Wright et al. [8] have shown that waste plastic can disintegrate into smaller shreds and can infiltrate into the human food chain. Another study by Browne et al. [9] has shown that the micro-sized plastic particles can pass on to human via fish. In fact, it has been found that about 60% to 80% of marine wastes are plastic. Statistics predicted that about 33 billion tons of plastic will be used by 2050, leading to serious environmental problems if this astronomic waste is incinerated or landfilled [10]. Face to this alarming situation, which will continue to increase, if any proper action is not taken, we are in urgent need to effective environmentally friendly methods to recover energy from waste plastics. The actual best technique is the pyrolysis of waste plastic to convert them into useful fuels [11].

The use of WPLO in a diesel engine is a recent research area and remains a subject under discussion. Soloiu et al. [12] conducted an experimental investigation of a single cylinder diesel engine with different WPLO fractions. He found that with increasing WPLO blends, in-cylinder pressure rises, however, peak pressures remain lower than that of diesel. Researchers [13-16] carried out some experimental studies on a single cylinder engine under various operating conditions. They used a WPLO fuel in various ignition timing and with cooled EGR. The research reported that the maximum heat release rate and in-cylinder peak pressure from WPLO are higher than that obtained from diesel. The results showed that BTE of WPLO blends is lower compared to that of diesel. Panda et al. [17] studied the effect of waste polypropylene oil as on the performances of a diesel engine. The results indicate that the BSFC is slightly lower with WPLO and WPLO-diesel blends. Kalargaris et al. [18] showed that the engine is able to operate stably with WPLO for long-term running at all engine loads without diesel addition.

Later, Kalargaris et al. [19] proved that polypropylene/diesel blends would be suitable for long-term use in a diesel engine at higher engine loads. The research showed that the most promising blend is considered to be 75% of polypropylene obtained at a pyrolysis temperature of 900 °C. According to researchers [18, 20], the pyrolysis temperature has a significant effect on combustion and emissions of diesel engines. The most obvious finding to emerge from this study is that the oil produced at a lower temperature (700 °C) presents higher brake thermal efficiency and shorter ignition delay period at all loads.

Most of the available literature studied the waste plastic oils derived from different plastic sources with various conversions technics however, which not extensively discussed is the usability of waste polyethylene oil as fuel for diesel engine. For this purpose, this work deals with an experimental investigation of Waste Polyethylene Oil called ‘WPO’, along with this paper, as an alternative fuel for a direct injection compression ignition engine. The effect of WPO fuel on performance and combustion parameters for a wide range of engine loads will be discussed. The present study fills a gap in the literature by integrating for the first time a numerical investigating of WPO behaviour as an alternative fuel for diesel engine. The conjunction of CFD with experiments helps to a better and profound analysis.

2. Experimental setup

2.1. Tested materials

The materials used in this study are Polyethylene wastes. The pyrolysis process is carried out in 4 stages: a) 5 minutes at 303 K, to eliminate any probable perturbation at the beginning of heating and to ensure the stability of the device. b) A heating ramp from 303 K to 973 K with a speed of 5 K/min, 10 K/min and 20 K/min. c) 5 min of heating at 973 K, for signal stabilization and the final step: d) Cooling from 973 K to 100 K with a speed of 50 K/min.

2.2. Engine test bench

The experimental engine used for this study was connected to an automatically controlled eddy current. The mean pressure, top dead centre position and injection pressure are processed with specific software providing the averaged in-cylinder pressure over 100 cycles. The pollutants analyser is connected to the engine exhaust manifold with a heated duct called a hotline for extracting exhaust gas samples to be analysed. The pressures, temperatures and engine mechanical parameters are measured using a low-frequency acquisition system running on a locally developed acquisition program. Table 1 summarizes various instruments used in this work with their sensitivity. The schematic of the test engine setup is shown in Fig. 1, and its specifications are shown in Table 2. Table 3 gives the properties of WPO and diesel fuels used.

3. Results and Discussion

The experimental tests are conducted at a stationary engine regime of 1500 rpm under various loads. The engine thermal equilibrium was reached before measures. The engine was sequentially fuelled with neat diesel to get its performances and then with WPO fuel. The results obtained from WPO are discussed and compared with the diesel fuel at the same operating conditions.

Table 1. Sensors measurements errors.

Measurements	Sensor type	Accuracy
Torque	Effort sensor (FN 3148)	$\pm 0.1 \text{ Nm}$
Speed	AVL 364C	$\pm 3 \text{ rpm}$
Injection timing	AVL 364C	$\pm 0.05 \text{ CA}$
Temperature of injected fuel	K type	$\pm 1.6 \text{ C}$
Temperature of exhaust gas	K type	$\pm 1.6 \text{ C}$
Temperature of ambient air	HD 2012 TC/150	$\pm 0.2 \text{ C}$
Cylinder pressure	Piezo-electric (AVL QH32D)	$\pm 2 \text{ bars}$
Injection pressure	Piezo-electric (AVL QH33D)	$\pm 2 \text{ bars}$
Fuel mass flow rate	Coriolis type (RHM015)	$\pm 0.5\%$
Intake air flow rate	Differential pressure transmitter (LPX5841)	$\pm 1.0\%$
HC	FID (Graphite 52 M)	$\pm 10 \text{ ppm}$
CO	Infra-red detector (MIR 2M)	$\pm 50 \text{ ppm}$
CO ₂	Infra-red detector (MIR 2M)	$\pm 0.2\%$
NOx	Chemiluminescence (TOPAZE 32M)	$\pm 100 \text{ ppm}$
Particulates	Electric (Pegasor particle sensor)	$\pm 1 \mu\text{g}/\text{m}^3$

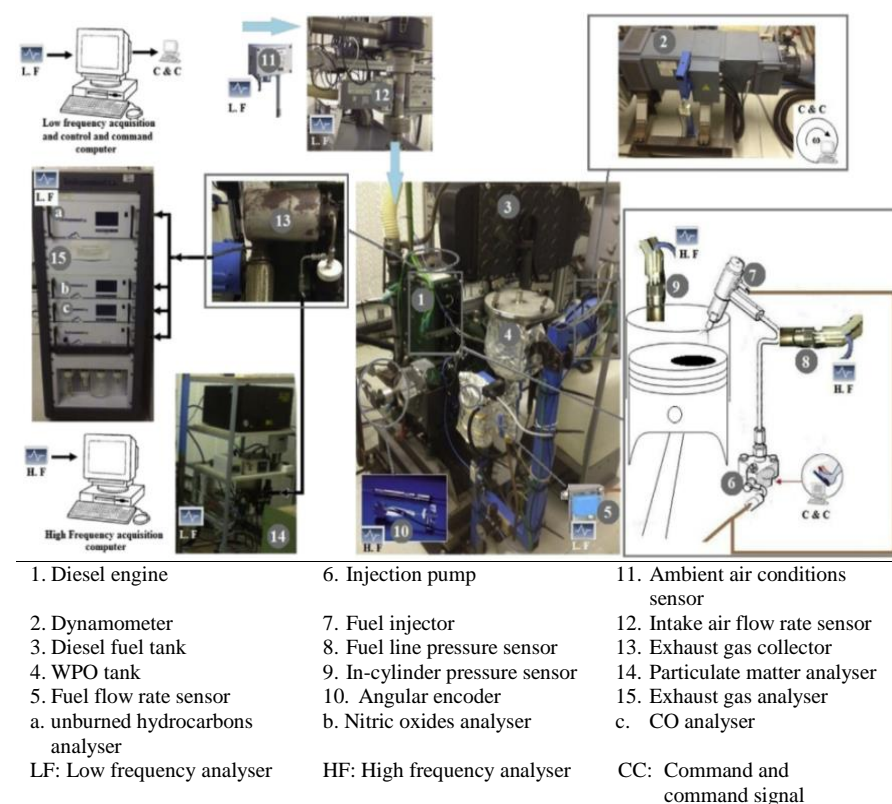
**Fig. 1. Schematic diagram of the test engine setup.**

Table 2. Engine technical specifications.

Specifications	
General details	Engine/Lister petter-TS 1 four-stroke, compression ignition, air-cooled, naturally aspirated, single-cylinder engine
Bore and stroke	95.3 mm × 88.9 mm
Connecting rod length	165.3 mm
Compression ratio	18:1
Maximum power	5.4 kW at 1800 RPM
Injector opening pressure	250 bars
Fuel injection timing	20 degrees BTDC

Table 3. Fuels properties.

Properties	ASTM standard method	WPO	Diesel
Density at 15 °C (kg/m³)	D4052-91	850	840
Kinematic viscosity at 40 °C (mm²/s)	D445	2.11	2.60
Lower heating value (MJ/kg)	D2015-85	45	42.9
Cetane number	D613	62	53
Oxygen content (wt %)	D5622	1.4	0.005
Flash point (°C)	D93-94	58	51
Pour point	D97	-7	-2/-12
Aromatic content (%)	IP 391	65.5	29.5

3.1. Combustion characteristics and engine performances

Figure 2 depicts the BSC at full load according to the engine rotational speed for both fuels. The BSC of neat diesel is higher than WPO at all regimes. The BSC of WPO rises from 21.3 g/min at 1500 to 34 g/min at 2400 rpm. The marginally enhance of WPO BSC comparing to neat diesel is due to higher LHV of WPO than that of neat diesel resulting in a reduction of mass flow rate of WPO. Figure 2 reveals also, that by increasing the power, BSC increases too because more fuel is required to generate additional engine torque to compensate loads [14, 17, 21]. The evolution of BTE with brake power for both fuels is presented in Fig. 3. Brake thermal efficiency in internal combustion engines measures the efficiency of the conversion of chemical energy of fuel into mechanical work output and it increases directly with load [22]. The increase of break power leads to an increase in BTE for both fuels. BTE of neat diesel show slightly lower efficiency, especially at low load. This indicates that WPO combustion is better than neat diesel due to its oxygen content and lower viscosity helping for a better mixture preparation. A slight drop of brake thermal efficiency of WPO fuel is observed when the engine brake power exceeds 3.5 kW due to higher heat transfer losses.

The evolution of exhaust gas temperature with the engine brake power for neat diesel and WPO fuels is shown in Fig. 4. It can be seen from this figure that the increase of the engine power leads to an increase in exhaust gas temperature for both fuels. At high load, the WPO exhaust gas temperature is lower than that of neat diesel. The reduction of temperature from WPO fuel confirms the higher heat transfer losses.

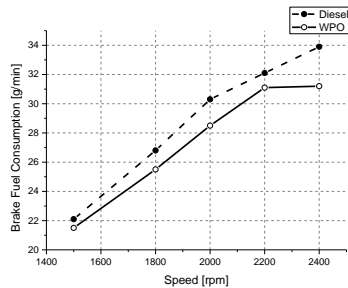


Fig. 2. Brake fuel consumption according to engine rotational speed.

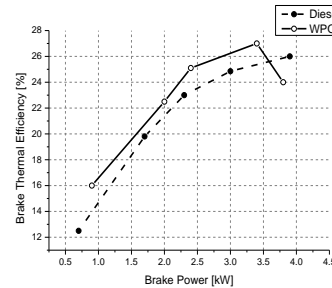


Fig. 3. Brake thermal efficiency according to engine brake power.

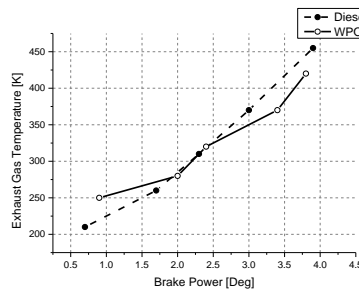


Fig. 4. Exhaust gas temperature versus engine brake power.

3.2. Emissions

Figure 5 depicts the variation of UHC emissions according to brake power for neat diesel and WPO. UHC emission increase according to load for both fuels. The incomplete fuel burning, the under mixing or over leaning zones and the wall flame-quenching are the main factors affecting the formation of UHC [18, 23, 24]. A substantial reduction of UHC emission is observed notably at medium load range for WPO confirming better combustion due to higher oxygen content and good atomization. However, at low and full loads the UHC emission of WPO are closer to those of net diesel due to improper mixing caused by local oxygen deficiency to burn the maximum injected fuel in the cylinder at high load, while at low load the UHC level is lower due to the oxygen abundance. For partial loads, due to the lower viscosity of WPO, the air/WPO mixing is better than that of air/diesel, which leads to better combustion quality [25]. The turbulence-combustion interaction is also the main responsible for high hydrocarbon emissions [26, 27].

Figure 6 illustrates the evolution of CO emissions. It can be seen that up to 2.5 kW, increasing engine brake power does not affect CO emissions for both fuels. However, besides the medium range, between 2.5 kW and 3.5 kW, the CO emissions are lower for WPO fuel. This confirms again the good quality of combustion in this power range comparing to the partial load operating conditions. The lower viscosity of WPO enhances the atomization and mixture preparation with air during the ignition delay period, which by the way enhances the oxidation of the carbon atoms [2]. CO emissions increase from 50 ppm at low engine power to 5500 ppm at 3.7 kW for net diesel. The same value is noticed for WPO fuel.

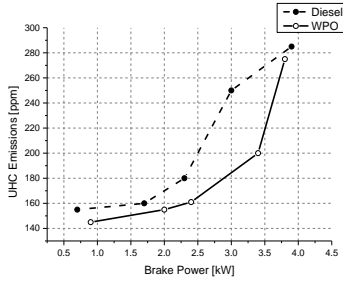


Fig. 5. UHC emissions according to brake power.

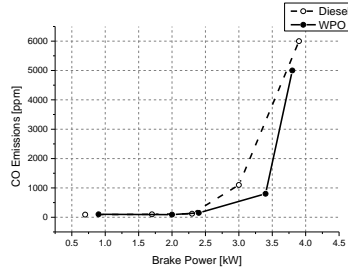


Fig. 6. CO emissions according to engine brake power.

Figure 7 presents the NO_x emissions according to the engine brake power. In diesel engines, NO_x emissions are formed by the thermal mechanism that requires high activation energy, coming mainly from the availability of oxygen and from the increase of in-cylinder temperature [18, 20, 23, 28]. At medium power range (2.5 Kw/3.5kW), NO_x emissions from WPO are higher. At low and full engine power operation, WPO presents relatively lower NO_x emissions due respectively to the lower in-cylinder temperatures and lower excess air.

Particulate Matter (PM) emissions measurements are presented in Fig. 8 according to the engine brake power. The analysis of these results show that the formation of carbon monoxide (Fig. 6) is directly proportional to PM formation; as well as the formation of NO_x, which is inversely proportional to PM formation. Figure 7 indicates the classical antagonism between NO_x and particles in diesel engines. At low loads, there are fewer emissions of carbon monoxide and therefore, less PM emissions. At high loads corresponding to rich mixtures, there is less oxygen to oxidize the formed carbon monoxide, which explains the increase in PM emissions and the decrease of NO_x [29].

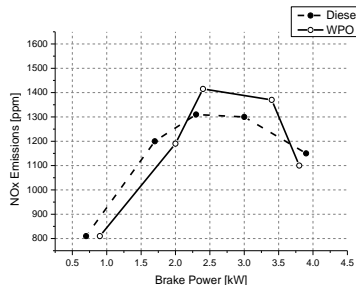


Fig. 7. NO_x emissions according to engine brake power.

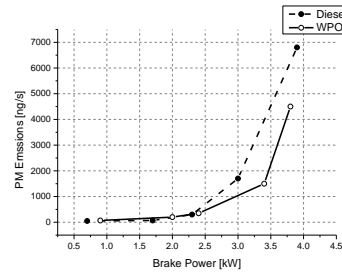


Fig. 8. Particles emissions according to engine brake power.

To summarize the main results of the previous experimental part, it can be noticed that in terms of mechanical and energy performance, the engine fuelled by WPO provides better results than those obtained with neat diesel. However, in terms of pollutant emissions, it appears that the WPO produces more NO_x than neat diesel in the operating range from 2.5 kW to 3.5 kW. The classic NO_x-PM duality problem persists with WPO.

4. Simulation Framework and Results

4.1. Numerical models

A numerical investigation on a three-dimensional in-cylinder domain is carried out under the CFD code Converge environment to get more detailed results. The classical governing equations of mass, momentum, energy, species are resolved with a RANS approach and the Redlich-Kwong equation of state is considered. Studies by Yue et al. [30] showed that the use of the real equation of state enhances the temperature prediction and hence the formation of soot, NOx and CO. The computational mesh for the engine combustion chamber with a base cell size of 2.4 mm is adopted. AMR technique refines the mesh based on temperature gradient, leading to a minimum mesh cell size of 0.6 mm.

Figure 9 gives the evolution of cells number in the computational domain according to the CA. The initial total cells at the start of the simulation are 49972 cells. The computational mesh contains a maximum of 656470 cells at 93 CA ATDC degrees, where the temperature gradient is largest on the computational domain due to the combustion process. An example of a 2.4 mm base cell with refinement at 23 CA ATDC degrees is illustrated in Fig. 10. Numerical simulations were performed in series on 5 cores and took approximately 32.83 hours for each fuel. From the total CPU time, 77.73% is used for solving the transport equations, while 16,29% is used to move surface and update grid.

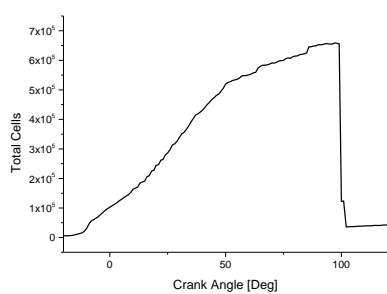


Fig. 9. Total mesh number during simulation.

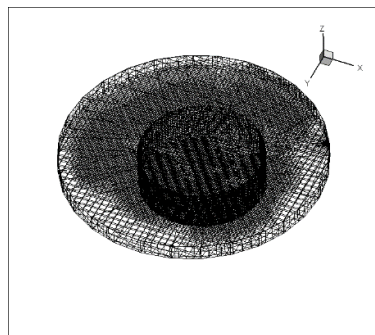


Fig. 10. Computational domain at 23 CA ATDC.

The thermo-physical properties of the liquid fuel are considered since the change in the liquid properties is very important for spray calculation (injection, breakup, collision, vaporization, etc.). For the liquid injection, a blob cone injection model with variable rate shape is used. The appropriate rate shape is shown in Fig. 11. In order to model the spray breakup, a modified KH-RT model is used. For the collision and coalescence modelling, the NTC (No Time Counter) model is used. The shell/CTC is used for combustion modelling. The model involves two sub-models: CTC and shell. The CTC model handles the conversion rate of the density of species at high-temperature reactions while Shell models the auto ignition process of diesel fuel [31]. For turbulence modelling, the rapid distortion RNG k-epsilon model is used. It is stated by Wang et al. [32], that model is designed for rapid compression or rapid expansion and therefore, it is well convenient for this case. In addition, the heat transfer wall model is used.

4.2. Simulation Results and Discussion

Results obtained from WPO fuel and neat diesel are compared at the same engine operating conditions (full load at 1500 rpm) for which, the fuel injection profile is illustrated in Fig. 11. Figure 12 shows the numerical and experimental in-cylinder pressure. Good agreement is achieved for both fuels. It is noticed that the simulation follows the measured pressure behaviour quite well and hence, justifying the convenient choice of the numerical models. The difference in the start of ignition between the measured and computed pressure for both fuels could be due to a minor underprediction in the in-cylinder temperature and pressure around the TDC as shown in the zoomed view of Fig. 12. The reason behind the misprediction of pressure and temperature may be due to the mechanism involved by the mixture formation and the spray atomization, which may result in a slight reduction in the temperature due to the absorption of heat during compression. The overprediction showed in the zoomed view of Fig. 12 may be due to the use of the RNG k- ϵ model, which apparently misrepresents the rate of mixing during combustion [33]. Maximum deviation between experiments and in-cylinder numerical pressures was 1.34 bars for neat diesel and 1.44 bars for WPO fuel, which represents about 1.5% for both fuels. For both numerical and experimental pressure, the peak pressure of net diesel fuel is higher over 1.525 bars than that of WPO because of the longer ignition delay of diesel fuel. Longer ignition delay increases the amount of flammable air/fuel mixture in the rapid combustion phase resulting in higher peak pressure. The peak pressure for both fuels occurs at 5 CA degrees ATDC.

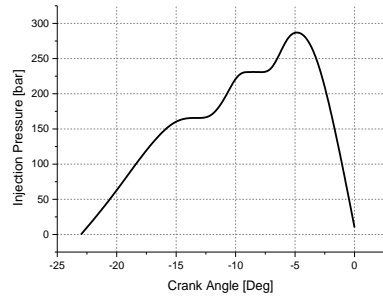
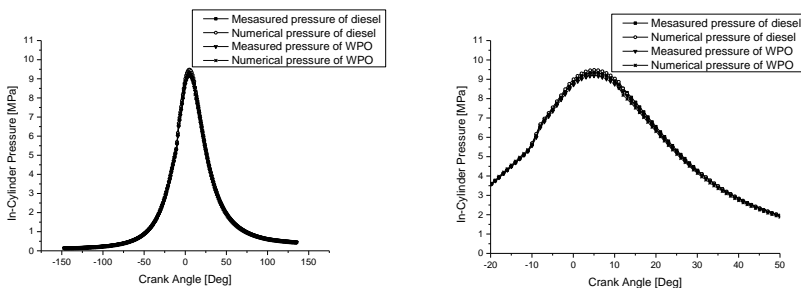


Fig. 11. Injection pressure profile (full load at 1500 rpm).



(a) Measured and numerical pressures. (b) Zoom in view around TDC.

Fig. 12. Evolution of in-cylinder pressure.

Figures 13 and 14 show respectively heat release rate and integrated heat release with crank angle. The heat release rate of the diesel engine is commonly subdivided into three phases: after the ignition delay period the premixed (or rapid) combustion phase occurs rapidly in few crank angle degrees (first pic), whereas the diffusion (or mixing-controlled) phase is the second pic, where the combustion is controlled by the availability of the burned mixture. This period involves various physical processes including atomization, vaporization and mixing of vapour fuel with air [23]. For both fuels, the main heat release period occurs in the diffusion combustion period and lasts at 60 CA degrees ATDC. The lower viscosity and high oxygen content of WPO lead to good atomization and mixture formation during the ignition delay period, which results in the earlier start of combustion as shown in Fig. 13.

Figure 15 shows the in-cylinder temperature for WPO and neat diesel. It can be seen that the in-cylinder mean temperature is higher for neat diesel confirming the experimental result shown in Fig. 4. The curves shown in Figs. 13 to 15 confirm newly the early start of heat release for WPO resulting in a shorter ignition delay compared to diesel. The in-cylinder temperature is directly affected by the ignition delay, longer ignition delay of diesel fuel delays the combustion and leads to higher exhaust gas temperature than that of WPO [34, 35].

Figure 16 shows the liquid penetration length. To measure LPL, the total mass of the liquid parcels is calculated from the nozzle then multiplies this mass by the liquid penetration fraction to yield the penetrated spray mass. Starting from the centre of the nozzle hole, Converge code sums the mass of the liquid parcels until it reaches the penetrated spray mass, which is LPL [36]. In the current simulation, LPL is set to 0.98 for both diesel and WPO. The spray of waste plastic fuel is more prolonged due to its lower viscosity. However, beyond 10 CA degrees BTDC, the LPL of neat diesel fuel is higher than WPO as shown in Fig. 16. This is due to the higher ignition delay of diesel fuel. In fact, longer ignition delay of neat diesel fuel achieves a further penetration of the spray in the combustion chamber.

CO emissions are as shown in Fig. 17 are an intermediate species of combustion and results from incomplete combustion [2]. They are primarily controlled by the fuel-air equivalence ratio [23]. The low viscosity of WPO enhances the atomization process resulting in a better locally fuel-air mixture, which contributes to less CO emissions production comparing to neat diesel fuel. Figure 18 presents the CO₂ emissions for WPO and diesel fuels. CO₂ is a greenhouse effect gas, hence, there is a strong requirement to be reduced [20].

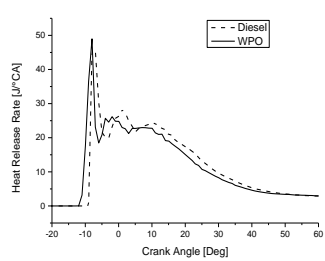


Fig. 13. Heat release rate.

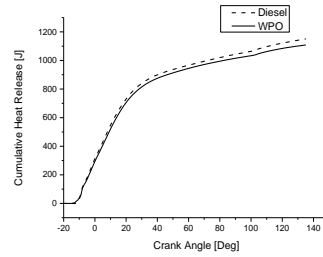
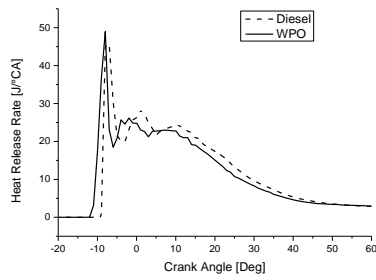
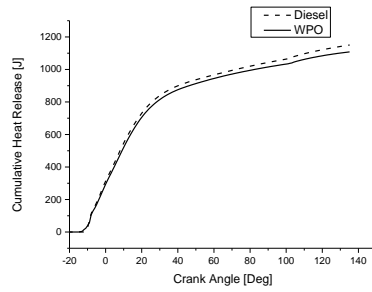
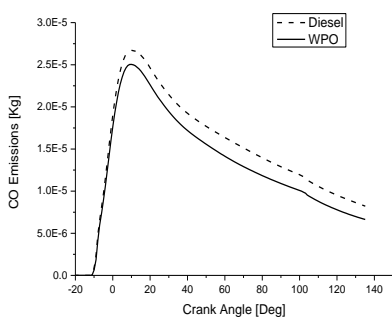
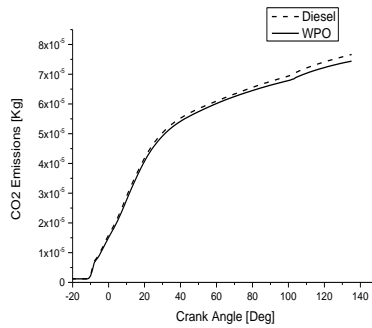


Fig. 14. Cumulative heat release.

**Fig. 15. Average in-cylinder temperature.****Fig. 16. Spray penetration.****Fig. 17. CO emissions.****Fig. 18. CO₂ emissions.**

CO₂ emissions from WPO are lower than that observed in neat diesel fuel and this is due to the enhancement of the BSFC, since less injected mass fuel is required for WPO fuel comparing to neat diesel at this load. Figure 19 depicts NO_x emissions, which are strongly depending on the local in-cylinder temperature. The higher in-cylinder temperature of diesel comparing to WPO leads to more NO_x emissions. This result confirms the experimental one shown in Fig. 7.

Figure 20 presents the unburned hydrocarbon emissions, which are produced from the incomplete combustion of hydrocarbon fuel and occur near the cylinder wall because, at this regions, the air-fuel mixture temperature is significantly lower [26]. The UHC emissions are produced in a faster manner during the rapid combustion phase. However, the rate of UHC production decline significantly during the mixing combustion period correspondingly to heat release rate during the same combustion period.

The soot emissions are depicted in Fig. 21 and reach their maximum at the end of the premixed combustion phase for both fuels. Soot emissions from WPO are lower comparing to neat diesel fuel. The lower viscosity and the presence of oxygen in the WPO chemical composition reduce the soot emissions. This result is also confirmed by the experimental one of Fig. 8.

Figure 22 illustrates the impact of injection timing on the in-cylinder pressure of WPO. It can be noticed that advancing injection timing leads to in-cylinder pressure growth. With advancing injection timing from 20 CA degrees BTDC to 30 CA degrees BTDC, the maximum in-cylinder pressure rises from 9.17 MPa to 10.60 MPa

corresponding to a gain of 10%. The enhancement of the in-cylinder pressure with advancing injection is due to lower ignition delay of WPO. When injection is earlier, a longer time is given to the atomization, evaporation and mixing process, which increases the rapid premixed combustion part leading to high heat release and higher peak pressure [23, 37]. Although at injection timing of 30 CA degrees BTDC corresponds to the higher peak pressure, however, the engine cannot operate at this condition for long-term use. The simulation results suggest advancing the ignition timing to obtain better performances but more numerical and experimental investigations are required to get the complete results. This is our future work.

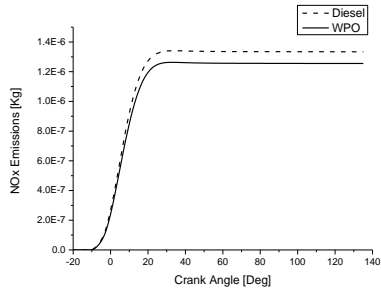
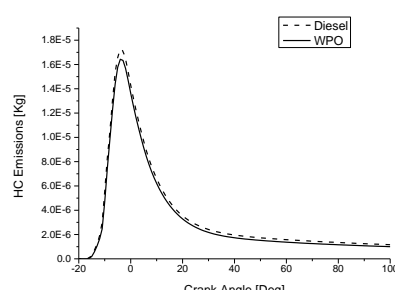
Fig. 19. NO_x emissions.

Fig. 20. HC emissions.

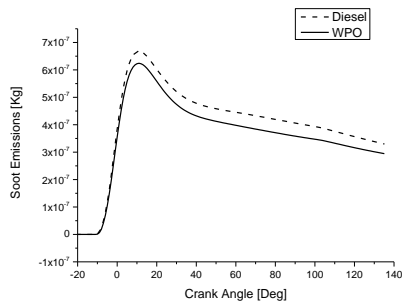


Fig. 21. Soot emissions.

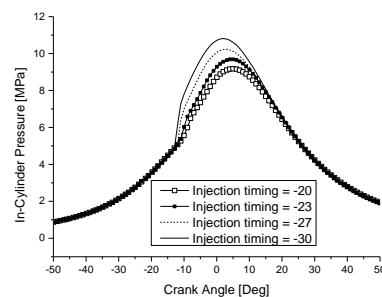


Fig. 22. Influence of injection timing on WPO in-cylinder pressure.

5. Conclusion

An experimental and numerical investigation was carried out to analyse the effects on the combustion and emission characteristics of a four-stroke, single cylinder, naturally aspirated, direct-injection diesel engine fuelled with oil derived from the pyrolysis of waste polyethylene at different operating conditions. The obtained results are compared to those obtained from neat diesel fuel at the same engine operating conditions. The following conclusions can be drawn:

- Total fuel consumption of WPO is lower than that of neat diesel fuel due to the higher LHV of WPO.
- BTE is improved for WPO especially at low load; however, beyond 3.5 kW the BTE for WPO shows a slight decline.
- The exhaust gas temperature is lower for WPO than that of diesel at low and full load.

- Ignition delay for WPO is less when compared to neat diesel fuel. The higher cetane number and lower viscosity of WPO enhance the air-fuel mixing decreasing consequently the delay period.
- At low load CO and particulate emissions from WPO doesn't affect while HC emissions are slightly higher for neat diesel. Interesting decreases of CO, UHC and PM emissions are obtained at medium loads. However, at this range, NO_x emissions found to be higher for WPO.
- Results from the numerical simulation show that the lower ignition delay and the advanced heat release rate at the premixed phase of WPO combustion are responsible for lower peak pressure and lower exhaust temperature levels. This is also confirmed by the spray penetration results.
- The simulation results suggest advancing the injection timing while running diesel engine with WPO.

Abbreviations

AMR	Adaptive Mesh Refinement
ATDC	After Top Dead Centre
BSFC	Break Specific Fuel Consumption
BTDC	Before Top Dead Centre
BTE	Brake Thermal Efficiency
CA	Crank Angle
CTC	Characteristic Time-scale Combustion model
EGR	Exhaust Gas Recirculation
HC	Hydrocarbons
HR	Heat Release
KH-RT	Kelvin-Helmholtz/Rayleigh-Taylor hybrid model
LHV	Lower Heating Value
LPL	Liquid Penetration Length
NTC	No Time Counter
PM	Particulate matter
ppm	Parts per million
PPO	Plastic Pyrolysis Oil diesel
SCR	Selective Catalytic Reduction
TDC	Top Dead Centre
TFC	Total Fuel Consumption
UHC	Unburned Hydrocarbon
WPLO	Waste Plastic Oil
WPO	Waste Polyethylene Oil

References

1. Das, P.; and Tiwari, P. (2018). Valorization of packaging plastic waste by slow pyrolysis. *Resources, Conservation and Recycling*, 128, 69-77.
2. Othman, M.F.; Adam, A.; Najafi, G.; and Mamat, R. (2017). Green fuel as alternative fuel for diesel engine: A review. *Renewable and Sustainable Energy Reviews*, 80, 694-709.

3. Plastics Europe. (2017). *Plastics Europe operation clean sweep report 2017*. Association of Plastics Manufacturers, Brussels, Belgium. 24 pages.
4. Plastics Europe. (2016). *Plastics - the facts 2016: An analysis of European plastics production, demand and waste data*. Association of Plastics Manufacturers, Brussels, Belgium. 35 pages.
5. Kassargy, C.; Awad, S.; Burnens, G.; Kahine, K.; and Tazerout, M. (2017). Experimental study of catalytic pyrolysis of polyethylene and polypropylene over USY zeolite and separation to gasoline and diesel-like fuels. *Journal of Analytical and Applied Pyrolysis*, 127, 31-37.
6. Jambeck, J.R.; Geyer, R.; Wilcox, C.; Siegler, T.R.; Perryman, M.; Andrady, A.; Narayan, R.; and Law, K.L. (2015). Plastic waste inputs from land into the ocean. *Science*, 347(6223), 768-771.
7. Owusu, P.A.; Banadda, N.; Zziwa, A.; Seay, J.; and Kiggundu, N. (2018). Reverse engineering of plastic waste into useful fuel products. *Journal of Analytical and Applied Pyrolysis*, 130, 285-293.
8. Wright, S.L.; Thompson, R.C.; and Galloway, T.S. (2013). The physical impacts of microplastics on marine organisms: A review. *Environmental Pollution*, 178, 483-492.
9. Browne, M.A.; Dissanayake, A.; Galloway, T.S.; Lowe, D.M.; and Thompson, R.C. (2008). Ingested microscopic plastic translocates to the circulatory system of the mussel, *Mytilus edulis* (L.). *Environmental Science and Technology*, 42(13), 5026-5031.
10. Rochman, C.M.; Browne, M.A.; Halpern, B.S.; Hentschel, B.T.; Hoh, E.; Karapanagioti, H.K.; Rios-Mendoza, L.M.; Takada, H.; Teh, S.; and Thompson, R.C. (2013). Policy: Classify plastic waste as hazardous. *Nature*, 494(7436), 169-171.
11. Kalargaris, I.; Tian, G.; and Gu, S. (2017). Combustion, performance and emission analysis of a DI diesel engine using plastic pyrolysis oil. *Fuel Processing Technology*, 157, 108-115.
12. Soloiu, V.A; Yoshihara, Y.; Nishiwaki, K.; Kako, T.; and Hiraoka, M. (2004). The development of a new emulsified alternative fuel for diesel power generation, produced from waste plastics. *Proceedings of the 24th World Congress of the International Council on Combustion Engines Technology (CIMAC)*, Kyoto, Japan, 14.
13. Mani, M.; and Nagarajan, G. (2009). Influence of injection timing on performance, emission and combustion characteristics of a DI diesel engine running on waste plastic oil. *Energy*, 34(10), 1617-1623.
14. Mani, M.; Subash, C.; and Nagarajan, G. (2009). Performance, emission and combustion characteristics of a DI diesel engine using waste plastic oil. *Applied Thermal Engineering*, 29(13), 2738-2744.
15. Mani, M.; Nagarajan, G.; and Sampath, S. (2010). An experimental investigation on a DI diesel engine using waste plastic oil with exhaust gas recirculation. *Fuel*, 89(8), 1826-1832.
16. Mani, M.; Nagarajan, G.; and Sampath, S. (2011). Characterisation and effect of using waste plastic oil and diesel fuel blends in compression ignition engine. *Energy*, 36(1), 212-219.

17. Panda, A.K.; Murugan, S.; and Singh, R.K. (2016). Performance and emission characteristics of diesel fuel produced from waste plastic oil obtained by catalytic pyrolysis of waste polypropylene. *Energy Sources, Part A: Recovery, Utilization, and Environmental Effects*, 38(4), 568-576.
18. Kalargaris, I.; Tian, G.; and Gu, S. (2017). The utilisation of oils produced from plastic waste at different pyrolysis temperatures in a DI diesel engine. *Energy*, 131, 179-185.
19. Kalargaris, I.; Tian, G.; and Gu, S. (2018). Experimental characterisation of a diesel engine running on polypropylene oils produced at different pyrolysis temperatures. *Fuel*, 211, 797-803.
20. Kalargaris, I.; Tian, G.; and Gu, S. (2017). Experimental evaluation of a diesel engine fuelled by pyrolysis oils produced from low-density polyethylene and ethylene - vinyl acetate plastics. *Fuel Processing Technology*, 161, 125-131.
21. Mohanraj, C.; Senthilkumar, T.; and Chandrasekar, M. (2017). A review on conversion techniques of liquid fuel from waste plastic materials. *International Journal of Energy Research*, 41(11), 1534-1552.
22. Dhinesh, B.; and Annamalai, M. (2018). A study on performance, combustion and emission behaviour of diesel engine powered by novel nano nerium oleander biofuel. *Journal of Cleaner Production*, 196, 74-83.
23. Heywood, J.B. (1988). *Internal combustion engine fundamentals (1st ed.)*. New York, United States of America: McGraw-Hill, Incorporated.
24. Greeves, G.; Khan, I.M.; Wang, C.H.T.; and Fenne, I. (1977). Origins of hydrocarbon emissions from diesel engines. *SAE Transactions*, 86(Section 2: 770189-770402), 1235-1251.
25. Boopathi, D.; Sonthalia, A.; and Devanand, S. (2017). Experimental investigations on the effect of hydrogen induction on performance and emission behaviour of a single cylinder diesel engine fuelled with palm oil methyl ester and its blend with diesel. *Journal of Engineering Science and Technology (JESTEC)*, 12(7), 1972-1987.
26. Chuah, L.F.; Aziz, A.R.A.; Yusup, S.; Bokhari, A.; Klemes, J.J.; and Abdullah, M.Z. (2015). Performance and emission of diesel engine fuelled by waste cooking oil methyl ester derived from palm olein using hydrodynamic cavitation. *Clean Technologies and Environmental Policy*, 17(8), 2229-2241.
27. Zheng, M.; Mulenga, M.C.; Reader, G.T.; Wang, M.; Ting, D.S.-K.; and Tjong, J. (2008). Biodiesel engine performance and emissions in low temperature combustion. *Fuel*, 87(6), 714-722.
28. Wei, L.; Cheng, R.; Mao, H.; Geng, P.; Zhang, Y.; and You, K. (2018). Combustion process and NOx emissions of a marine auxiliary diesel engine fuelled with waste cooking oil biodiesel blends. *Energy*, 144, 73-80.
29. Kuncser, R. (2011). *Contribution à l'étude de la production et de la combustion en moteur Diesel d'huiles de pyrolyse de déchets thermoplastiques*. Ph.D. Thesis. Polytechnic School of University of Nantes, Nantes, France.
30. Yue, Z.; Hessel, R.; and Reitz, R.D. (2018). Investigation of real gas effects on combustion and emissions in internal combustion engines and implications for development of chemical kinetics mechanisms. *International Journal of Engine Research*, 19(3), 269-281.

31. Kong, S.-C.; and Reitz, R.D. (1993). Multidimensional modeling of diesel ignition and combustion using a multistep kinetics model. *Journal of Engineering for Gas Turbines and Power*, 115(4), 781-789.
32. Wang, F.; Reitz, R.D.; Pera, C.; Wang, Z.; and Wang, J. (2014). Application of generalized RNG turbulence model to flow in motored single-cylinder PFI engine. *Engineering Applications of Computational Fluid Mechanics*, 7(4), 486-495.
33. Guo, C.; Song, Y.; Feng, H.; Zuo, Z.; Jia, B.; Zhang, Z.; and Roskilly, A.P. (2018). Effect of fuel injection characteristics on the performance of a free-piston diesel engine linear generator: CFD simulation and experimental results. *Energy Conversion and Management*, 160, 302-312.
34. Ndayishimiye, P.; and Tazerout, M. (2011). Use of palm oil-based biofuel in the internal combustion engines: Performance and emissions characteristics. *Energy*, 36(3), 1790-1796.
35. Kumar, M.S.; Kerihuel, A.; Bellette, J.; and Tazerout, M. (2006). A comparative study of different methods of using animal fat as a fuel in a compression ignition engine. *Journal of Engineering for Gas Turbines and Power*, 128(4), 907-914.
36. Richards, K.; Senecal, P.; and Pomraning, E. (2014). Converge (v2. 2.0). *Theory Manual, Convergent Science*, Madison, Wisconsin, United States of America.
37. Merker, G.P.; Schwarz, C.; Stiesch, G.; and Otto, F. (2006). *Simulating combustion: Simulation of combustion and pollutant formation for engine-development* (1st ed.). Berlin, Heidelberg: Springer-Verlag Berlin Heidelberg.